Application of the Random Coupling Model to Electromagnetic Statistics in Complex Enclosures

Zachary B. Drikas, *Member, IEEE*, Jesus Gil Gil, Sun K. Hong, *Member, IEEE*, Tim D. Andreadis, Jen-Hao Yeh, *Member, IEEE*, Biniyam T. Taddese, *Member, IEEE*, and Steven M. Anlage, *Member, IEEE*

***Abstract*—The effectiveness of the random coupling model (RCM) in predicting electromagnetic wave coupling to targeted electronic components within a complex enclosure is examined. In the short-wavelength limit with respect to the characteristic length of the enclosure, electromagnetic wave propagation within a large enclosure is sensitive to small changes to the interior, or to the boundaries of the enclosure. Such changes can reduce or invalidate the applicability of deterministic predictions of the electromagnetic fields at radiofrequencies (RF) in large enclosures. Under such circumstances, a statistical approach is needed to provide a better understanding of RF coupling to components within large enclosures. In this paper, we experimentally demonstrate the applicability of a statistical technique, the RCM, to estimate the probabilistic magnitudes of RF fields on electrically large components (i.e., long cables, etc.) that are partially shielded within a complex, 3-D enclosure.**

***Index Terms*—Electromagnetic compatibility (EMC), overmoded enclosures, probability density function, random coupling model (RCM), statistical electromagnetism, wave scattering.**

I. Introduction

There is practical interest in the statistics of electromagnetic radiation affecting sensitive electronics that are shielded within a large enclosure, both in areas of electromagnetic compatibility (EMC) [1]–[6], and in defense-related radiofrequency (RF) attack scenarios. The RF coupling to targeted electronics within a large enclosure can be studied by considering a wave scattering problem in the short-wavelength limit. While the applied wavelength is short with respect to the characteristic length of the wave enclosure, electromagnetic field distributions in electrically large enclosures can vary dramatically even with a small rearrangement of the internal objects, a small change in the enclosure boundaries, or a change in frequency of the excitation waveform. At a particular location, the field may have contributions from a superposition of hundreds of excited modes [4], and therefore, the locations of field maximums and minimums are also very sensitive to such small changes. Power coupling of electromagnetic fields to a component, such as a conductor or an electronic device, in one enclosure may be quite different in another nearly identical enclosure. Therefore, deterministic calculations are valid only for the particular situation modeled. Under such circumstances, analysis of the statistical properties of electromagnetic fields in these complex environments is necessary, and the statistical predictions can better represent the properties of complex enclosures.

The statistical treatment of electromagnetic fields in cavities (wave enclosures) is a well-researched area beginning with Holland and St. John [7]. Traditionally, statistical electromagnetic techniques involve determining the electric field intensity at a particular location in a cavity or determining the overall field distribution in order to evaluate shielding effectiveness or to determine the EMC of devices. The technique described in this study does not determine statistical field strengths, but rather takes an "impedance approach" to calculate induced voltages on ports in a complex enclosure. These ports can be a traditional antenna like a monopole, pins on an integrated circuit, or wires or bundles of wires running inside a below-deck ship compartment. The statistical coupling of RF energy to wires and wire bundles has been approached with other techniques. For example, Langley adapts a vibroacoustic method, which breaks the coupling problem into random and deterministic components that can be analyzed separately: the wire is taken to be the deterministic component and the surrounding dielectric cavity the random component [8]. In this paper, the statistical treatment is the random coupling model (RCM) that is based on wave chaos and has been successfully applied to describe the statistics of many wave scattering properties [9]–[11]. Wave chaos is a field that studies wave propagation in ray-chaotic enclosures in the short-wavelength limit [6], [12]. A ray-chaotic enclosure means the dynamics of the ray trajectories in the enclosure is chaotic, so initial deviations of trajectories grow, on average, exponentially in time [13]. In a wave chaotic system, the statistical features of wave scattering properties have a universal fluctuation part and a system-specific deterministic part. The universal fluctuation part is well-predicted by random matrix theory (RMT) [14], and the RCM combines the system-specific deterministic part with the universal fluctuation part in an impedance approach [15], [16]. It

Manuscript received July 15, 2013; revised April 9, 2014 and November 26, 2013; accepted May 22, 2014. Date of publication September 9, 2014; date of current version December 11, 2014. This work was supported by the ONR Applied Electromagnetics Program N0001410WX20844, the ONR/Maryland Applied Electromagnetics Center under Grant N0 0014-09-1-1190, Task A2, and ONR MURI through Grant N00014-07-1-0734.

Z. B. Drikas, J. G. Gil, S. K. Hong, and T. D. Andreadis are with the Department of Tactical Electronic Warfare Division, Naval Research Laboratory, Washington, DC 20375 USA (e-mail: zachary.drikas@nrl.navy.mil; jesus.gilgil@nrl.navy.mil; sun.hong@nrl.navy.mil; tim.andreadis@nrl.navy.mil).

J.-H. Yeh, B. T. Taddese, and S. M. Anlage are with the Department of Physics, University of Maryland, College Park, MD 20742 USA (e-mail: davidyeh@umd.edu; bini01@umd.edu; anlage@umd.edu).

Color versions of one or more of the figures in this paper are available online at http://ieeexplore.ieee.org.

Digital Object Identifier 10.1109/TEMC.2014.2337262

is conjectured that this wave chaos model, the RCM, can be applied to complex wave enclosures that are complicated enough in the short-wavelength limit such that the universal fluctuation feature is valid.

Previously, the RCM has been applied to predict RF field coupling through antennas of subwavelength dimension, into a quasi-2-D, ray-chaotic microwave cavity, [9], [11], [17], and a 3-D computer box [9], [11]. This paper extends the work of Hemmady *et al.* by examining the applicability of the RCM to a large, complex cavity, which has a short monopole antenna and a long antenna that is much larger than the wavelength. The short antenna represents a wave transmitting port. The long antenna is a 0.92-m long U-shaped conductor used as a receiving port and it represents a long piece of cable, or a bundle of wires, which could lead to a below-deck ship compartment that could be susceptible to picking up unwanted RF radiation. This could be useful for predicting damage due to an RF attack. The RCM has never been tested in the wave system with a multiple-wavelength-long port. Additionally, this study presents novel results, which show that the RCM predictions of induced voltages on a receiving port are independent of the transmitting port location.

This paper is organized as follows. In Section II, the theoretical approach of the RCM is briefly summarized. Section III details the experimental setup, and how the loss parameter (α) of the cavity is experimentally determined. The loss parameter determines the statistical distributions predicted by RMT and will be further introduced. Section IV presents experimental results that show that the RCM is applicable to a complex 3-D cavity, with an electrically large receiver port. The following four results are obtained: 1) the universal fluctuation part of the experimental data agrees with the prediction of RMT; 2) the system-specific feature can be described by the RCM; 3) the RCM prediction of the probability density function (PDF) of induced voltages on the long port matches the experimental data; and 4) the distribution of induced voltages on the electrically large port is independent of the transmitting port location. Finally, Section V summarizes the implications of these results.

II. Theory

The RCM is a statistical model that combines universal statistical properties of a wave chaotic system with system-specific features of the system to predict statistical properties of electromagnetic fields in a complex enclosure. The RCM is derived in the impedance domain and can predict the statistics of the impedance matrix and the scattering matrix of the system. Most importantly for the applications of EMC, the RCM predicts the PDF of induced voltages on target objects (ports) inside a complex enclosure [9], [11].

We are interested in comparing these predicted induced voltage PDFs with experimentally determined PDFs. The experimental-induced voltage is calculated from elements of the impedance matrix, which describes the linear relationship between the voltages at the ports and the currents at the ports. The measurement of a multiport complex cavity is typically carried out by obtaining the scattering matrix, $\boldsymbol{S}$, which may be transformed to an equivalent impedance matrix, $\boldsymbol{Z}$, obtained through the standard bilinear relationship

$$\boldsymbol{Z} = \boldsymbol{Z}_0^{1/2}(\boldsymbol{I}+\boldsymbol{S})(\boldsymbol{I}-\boldsymbol{S})^{-1}\boldsymbol{Z}_0^{1/2} \tag{1}$$

where $\boldsymbol{Z}_0$ is a diagonal matrix of the characteristic impedances of the waveguides connected to the ports of the cavity and $\boldsymbol{I}$ is the unit matrix. For a two-port system, all of these matrices are 2×2 matrices. Hart *et al.* show that the statistics of the impedance matrix, $\boldsymbol{Z}_{\rm cav}$, of a multiport complex cavity can be decomposed into parts that describe the *universal* (fluctuating) and *system-specific* (deterministic) properties of the cavity as [17], [18],

$$\boldsymbol{Z}_{\rm cav} = j\,{\rm Im}[\langle \boldsymbol{Z}_{\rm cav}\rangle] + {\rm Re}[\langle \boldsymbol{Z}_{\rm cav}\rangle]^{1/2}\boldsymbol{z}{\rm Re}[\langle \boldsymbol{Z}_{\rm cav}\rangle]^{1/2}. \tag{2}$$

The matrix $\langle \boldsymbol{Z}_{\rm cav}\rangle$ is called the ensemble-averaged cavity impedance matrix, which captures the system-specific features of the cavity [17]. Re[$\cdot$] and Im[$\cdot$] mean taking the real part and the imaginary part, respectively. The ensemble-averaged impedance matrix $\langle \boldsymbol{Z}_{\rm cav}\rangle$ is calculated by taking the average of the impedance matrices $\boldsymbol{Z}_{\rm cav}$ over a finite number of configurations of the cavity. In this paper, we measured 200 different 2×2 impedance matrices [obtained from the cavity scattering matrices using (1)], and the technique for generating different configurations of the cavity is discussed in Section III-A.

According to the RCM and previous experimental verifications [17], [18], $\langle \boldsymbol{Z}_{\rm cav}\rangle$ approximates the radiation impedance matrix, $\boldsymbol{Z}_{\rm rad}$, plus the short-trajectory coupling between the ports. The matrix $\boldsymbol{Z}_{\rm rad}$ represents the radiation and near-field characteristics of the ports, and can be measured by retaining the near-field properties of the port and establishing boundary conditions so that no waves ever return to the port (i.e., placing absorber on the walls of a cavity); $\boldsymbol{Z}_{\rm rad}$ can also be calculated. The short-trajectory coupling refers to either line-of-sight contributions between two ports or contributions made by ray trajectories that have made a few reflections inside the enclosure before coupling to the port [17], [18]. Both the radiation impedance matrix and the short-trajectory coupling are system-specific features, and are included in $\langle \boldsymbol{Z}_{\rm cav}\rangle$.

On the other hand, the universal fluctuating part is called the normalized impedance matrix

$$\boldsymbol{z} = ({\rm Re}[\langle \boldsymbol{Z}_{\rm cav}\rangle])^{-1/2}(\langle \boldsymbol{Z}_{\rm cav}\rangle - j{\rm Im}[\langle \boldsymbol{Z}_{\rm cav}\rangle])\,({\rm Re}[\langle \boldsymbol{Z}_{\rm cav}\rangle])^{-1/2} \tag{3}$$

whose statistical properties are predicted by the RMT. The normalized impedance matrix describes the universal fluctuation properties of the measured impedance $\boldsymbol{Z}_{\rm cav}$ [15], [16]. The statistics of all of the elements of the matrix $\boldsymbol{z}$ only depend on the loss parameter, α, of the system [9], [11]. The definition of the loss parameter and how to determine α by using experimental data will be further discussed in Section III-B. In a short summary, the RCM can model the statistics of $\boldsymbol{Z}_{\rm cav}$ by using the measured system-specific feature $\langle \boldsymbol{Z}_{\rm cav}\rangle$ and the statistical properties of $\boldsymbol{z}$, which is obtained by using the RMT and the single parameter, α. Consequently, the RCM can predict the statistics of the induced voltages on a target in a wave chaotic enclosure. The result is shown in Section III-C.

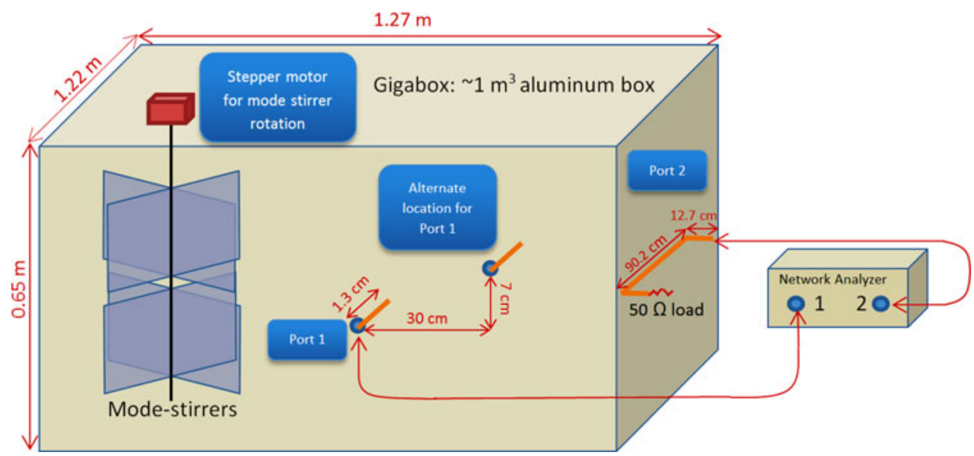

Fig. 1. Schematic diagram of the experimental setup. The GigaBox has mode-stirrers which are rotated with a LabVIEW controlled stepper motor. It has two ports that are connected to a network analyzer. The network analyzer operation is integrated with the LabVIEW control program. Port 2 is a U-shaped conductor whose other end is terminated with a 50-Ω load. There is an alternative location, on the wall of the GigaBox, to mount the transmitting port (port 1).

III. Experimental Setup and Data Analysis

A. Experimental Setup

We test the application of the RCM in modeling the wave coupling to targeted electronic components within a complex enclosure, which is shown in Fig. 1. The complex enclosure, called the GigaBox, is a reverberation chamber (rectangular aluminum box with dimensions of 1.22 m $\times$ 1.27 m $\times$ 0.65 m). There are mode stirrers (scatterers) made of aluminum inside the GigaBox, and the mode stirrers can be systematically rotated to 200 discrete orientations. It also has an irregular internal surface. The mode stirrers and the irregularities on the internal surface facilitate the creation of ray-chaotic trajectories inside the enclosure, and the elimination of degenerate modes.

The GigaBox has two ports. Port 1 is a monopole antenna with a physical length of 1.3 cm. The monopole antenna is internally mounted on a vertical wall of the GigaBox. Port 2 is a U-shaped conductor representing a long cable. The U-shaped conductor is a copper tube of 0.6-cm diameter. It is internally mounted on another wall of the GigaBox, which is orthogonal to the wall that carries the monopole antenna (port 1). The U-shaped conductor has a total length of 115.6 cm, and it has a 90.2-cm long portion that is parallel to the wall of the GigaBox at a distance of 12.7 cm from the wall. One end of the U-shaped conductor (port 2) is terminated with a 50-Ω load while the other end is connected to a network analyzer, and port 1 is also connected to the network analyzer as shown in the Fig. 1. The network analyzer measures the scattering matrix of the GigaBox as a 2×2 matrix, whose elements (denoted as S_{11}, S_{12}, S_{21}, and S_{22}) are complex functions of source frequency.

A large number of configurations of the cavity are required to achieve a randomized electromagnetic environment [19]. The mode stirrers inside the GigaBox are rotated to 200 different orientations to create 200 configurations of the GigaBox. These configurations of the GigaBox have the same volume and quality factor; however, their boundary conditions are different. Experiment has taught us that it is actually much fewer than 200 samples needed to provide a sufficient statistical ensemble, but we had the physical capability to have 200 realizations, so we used that amount. The scattering matrix is measured for each configuration over the frequency range 3–10 GHz, where the wavelength λ is small compared to the enclosure size. (A rule of thumb is to use $\lambda \ll \sqrt[3]{V}$, where V is the volume of the enclosure.) In the short-wavelength limit, there is significant perturbation between each configuration, and an autocorrelation analysis showed that the 200 measured realizations are highly uncorrelated samples.

B. Determination of the Loss Parameter of the GigaBox

As described in Section II, determination of the loss parameter of the cavity is essential to apply the RCM. In the frequency spectra of the transmitted or reflected signals of a complex wave enclosure, one can see separately distributed resonances over the measured frequency window. The dimensionless loss parameter, α, is defined as the ratio of the 3-dB (half-power) bandwidth of the closed-cavity mode resonance to the mean spacing between cavity modes (eigenmodes), $\alpha \equiv f/(2Q\Delta f)$. Here, f is the frequency, Δf is the mean spacing of adjacent eigenfrequencies, and Q is the typical (unloaded) quality factor of the cavity, which may be measured in several ways, one of which is to use $Q = 2\pi f \tau$, where $1/\tau$ is the rate of voltage decay in the cavity. The mean spacing of the eigenmodes may also be measured directly from the S_{21} (transmission) response of the cavity. Note that α is independent of the ports and is a property of the closed cavity which has eigenmodes and eigenfunctions dictated by the solutions of the wave equation. For an open system, such as the GigaBox, where waves access the enclosure from outside, we consider an equivalent closed system in which uniform absorption accounts for wave energy lost from the system, and we assume that we can define an equivalent loss parameter for the open system [9], [11].

The loss parameter, α, is the only parameter needed to describe the statistics of the universal properties of a wave-chaotic system. Hemmady has discussed several different methods for determining α in Appendix B of his thesis [9]. For example,

TABLE I
LOSS PARAMETER (α) IN DIFFERENT FREQUENCY WINDOWS

Frequency Range (GHz)	3.0 – 3.1	4.0 – 4.1	5.0 – 5.1	6.0 – 6.1	7.0 – 7.1	8.0 – 8.1	9.0 – 9.1	10.0 – 10.1
α	1.24	1.38	2.33	4.51	6.19	7.99	9.31	10.93

α can be calculated directly from first principles as

$$\alpha = \frac{k^3 V}{2\pi^2 Q} \tag{4}$$

in a 3-D cavity, where k is the wave number, V is the cavity volume, and Q is average cavity quality factor. This method works well when one knows or can estimate Q and V. Another method is to compare PDFs of the real and imaginary parts of the experimental normalized impedance matrix, $\boldsymbol{z}$, with the predicted PDFs of the RMT by using α as a fitting parameter [9], [17].

Instead of comparing the whole PDF, when the loss is high enough ($\alpha > 1$), α can be estimated by only using the variance of elements of the normalized impedance matrices, $\boldsymbol{z}$, from different configurations of the cavity [9], [20]. For example, the relationship of the variance of the off-diagonal elements of $\boldsymbol{z}$ and the loss parameter is

$$\alpha = \frac{1}{2\pi\sigma^2_{\mathrm{Re}[z_{ij}]}} = \frac{1}{2\pi\sigma^2_{\mathrm{Im}[z_{ij}]}}. \tag{5}$$

Here, σ^2 is the variance, $\mathrm{Re}[z_{\mathrm{ij}}]$ and $\mathrm{Im}[z_{\mathrm{ij}}]$ denote the real and imaginary parts of the off-diagonal components of the 2×2 normalized impedance matrix, $\boldsymbol{z}$. We refer to this method used to determine the loss parameter as "*the variance method,*" and it is the method used in this paper. Values of α obtained by the variance method are presented in Table I.

The loss parameter, α, is a smoothly varying function of frequency and is not expected to vary widely over small bandwidths such as 100 MHz as chosen in Table I. For a 100-MHz window, the average number of resonances is from 800 (in 3.0–3.1 GHz) to 8800 (in 10.0 – 10.1 GHz), and the number of points is set as 16 001 for the network analyzer.

IV. EXPERIMENTAL RESULTS

A. Applicability of the RMT to Universal Fluctuations in the GigaBox

We first examine the statistics of the normalized impedance matrix [$\boldsymbol{z}$ in (3)] to see if they agree with the predictions of the RMT. In order to carry out the normalization, the matrix $\langle \boldsymbol{Z}_{\mathrm{cav}} \rangle$ was computed by taking the average of the measured $\boldsymbol{Z}_{\mathrm{cav}}$ matrices over the 200 configurations; these $\boldsymbol{Z}_{\mathrm{cav}}$ matrices were obtained from scattering matrix measurements. Next, the normalized impedance, $\boldsymbol{z}$, was determined for each of the 200 measured $\boldsymbol{Z}_{\mathrm{cav}}$ matrices by solving (3).

Each of these $\boldsymbol{z}$ matrices has complex diagonal elements. The PDFs of the real and imaginary parts of these diagonal elements are shown in Fig. 2. In Fig. 2, the PDFs, which were generated solely from the experimental data, are compared with PDFs, which were generated using the RMT.

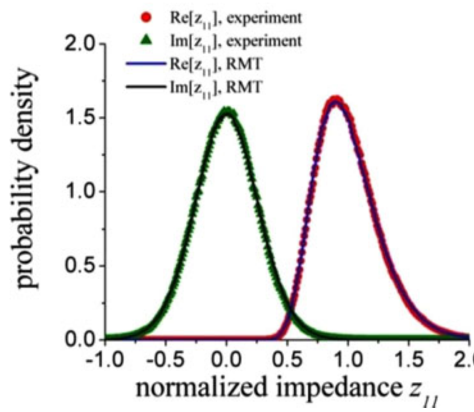

Fig. 2. PDFs of the real and imaginary parts of z_{11} generated experimentally (red circular labels and green triangular labels) and numerically (blue and black curves) for the frequency range 6.0–6.1 GHz. The distribution of the imaginary part has a zero mean and is symmetric while the distribution of the real part is not.

The RMT offers a Monte Carlo method to generate random impedance matrices, $\boldsymbol{z}_{\mathrm{RMT}}$, whose statistics are the same as the statistics of the normalized impedance matrix, $\boldsymbol{z}$. The random matrix can be generated as [9], [11]

$$\boldsymbol{z}_{\mathrm{RMT}} = \frac{-j}{\pi} \boldsymbol{W}(\boldsymbol{\Lambda} - j\alpha \boldsymbol{I})^{-1} \boldsymbol{W}^{\mathrm{T}} \tag{6}$$

where Λ is the random matrix of resonances (eigenmodes of the closed system), $\boldsymbol{I}$ is the unit matrix with the same size as Λ, and $\boldsymbol{W}$ is the random matrix of the port coupling. $\boldsymbol{W}^{\mathrm{T}}$ is the transpose matrix of $\boldsymbol{W}$. To represent an overmoded wave system, such as the complex enclosure in the short-wavelength limit, one needs to generate Λ as a large $M \times M$ matrix, where M is the number of eigenmodes and $M > 1000$. $\boldsymbol{W}$ is also a numerical generated random matrix with the size $N \times M$, where N is the number of ports. The rules of generating the random matrices Λ and $\boldsymbol{W}$ are indicated by the RMT [9], [14], [16], and they are out of scope of this paper. Note that the loss parameter α is the only parameter determining the statistics of the elements of $\boldsymbol{z}_{\mathrm{RMT}}$.

Fig. 2 shows PDFs of the real and imaginary parts of z_{11} for both experimental and theoretical (RMT) impedance data. The experimental data are from 6.0 to 6.1 GHz in the 200 configurations, and the theoretical data are numerically generated with the estimated loss parameter $\alpha = 4.51$. We use the Monte Carlo method to generate 2×10^6 impedance matrix samples. The distributions for the real parts of z_{11} (experimental and theoretical) are centered at one, and the distributions for the imaginary parts of z_{11} (experimental and theoretical) are centered at zero. This is what would be expected since $\boldsymbol{z}$ is the normalized impedance, and on average, the port reactance should be zero, which is consistent with the RCM. The experimental and theoretical PDFs show very good agreement. Note that only one parameter (α) is used to fit the PDFs. This demonstrates the applicability of the

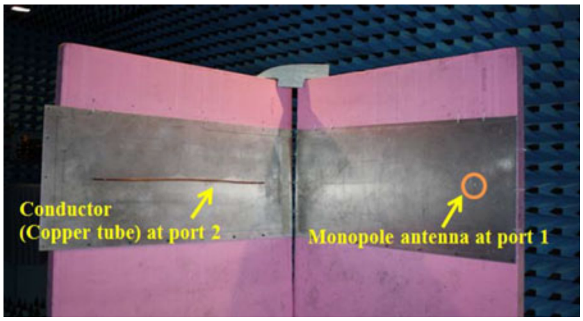

Fig. 3. Setup of free space radiation measurement.

RMT in describing the universal properties of a complex 3-D enclosure, which has an electrically large port.

B. Radiation Scattering of the GigaBox, $\boldsymbol{S}_{\rm rad}$

The radiation scattering matrix, which is denoted as $\boldsymbol{S}_{\rm rad}$, of the GigaBox was obtained by a free space measurement of the scattering matrix. The source frequency for the measurement was from 3 to 10 GHz. The free space radiation setup for the GigaBox was done by placing the GigaBox in an anechoic chamber, and removing all of its walls except for the two walls that are used to mount the two antennas (see Fig. 3). The setup is such that there is free space radiation between the two ports while closely maintaining near-field characteristics of the ports. The side walls used in our $\boldsymbol{S}_{\rm rad}$ measurement, Fig. 3, were finite in size, however, numerical simulation showed that the frequency characteristics were unperturbed. Comparing with the setup in Fig. 1, the short-trajectory coupling, which represents the short trajectories bouncing in the enclosure, is removed from the free space measurement of $\boldsymbol{S}_{\rm rad}$.

The ensemble-average matrix $\langle \boldsymbol{S}_{\rm cav} \rangle$ was calculated by averaging 200 cavity scattering matrices, which are measured in the cavity shown in Fig. 1. Fig. 4 shows the comparison between the magnitudes of $\boldsymbol{S}$ matrix elements (i.e., $|S_{11}|$, $|S_{22}|$, and $|S_{12}|$) of $\boldsymbol{S}_{\rm rad}$ and $\langle \boldsymbol{S}_{\rm cav} \rangle$ over the frequency range from 3 to 10 GHz. As predicted by the RCM, the radiation scattering elements, which represent the system-specific feature of the ports, follow the trend of the ensemble-averaged elements [10], [16]. The deviation between $\boldsymbol{S}_{\rm rad}$ and $\langle \boldsymbol{S}_{\rm cav} \rangle$ can be understood as the short-trajectory coupling effect introduced by Hart *et al.* [17], [18]. $\langle \boldsymbol{S}_{\rm cav} \rangle$ combines the radiation scattering matrix, $\boldsymbol{S}_{\rm rad}$, and the effects of short trajectories remaining after the ensemble average. Previous work on the RCM [17], [18] has examined the effects of utilizing either $\boldsymbol{S}_{\rm rad}$ or $\langle \boldsymbol{S}_{\rm cav} \rangle$ to convert to an impedance matrix and do the impedance normalization [see (3)]. Generally, utilizing $\langle \boldsymbol{S}_{\rm cav} \rangle$ makes the RCM more complete in describing the system and brings about better results in statistical predictions. The improvement is significant when the measured frequency range is small and cannot cover the corresponded frequency range of the shortest trajectory. Therefore, in this paper, we only use $\langle \boldsymbol{S}_{\rm cav} \rangle$ for the RCM analysis.

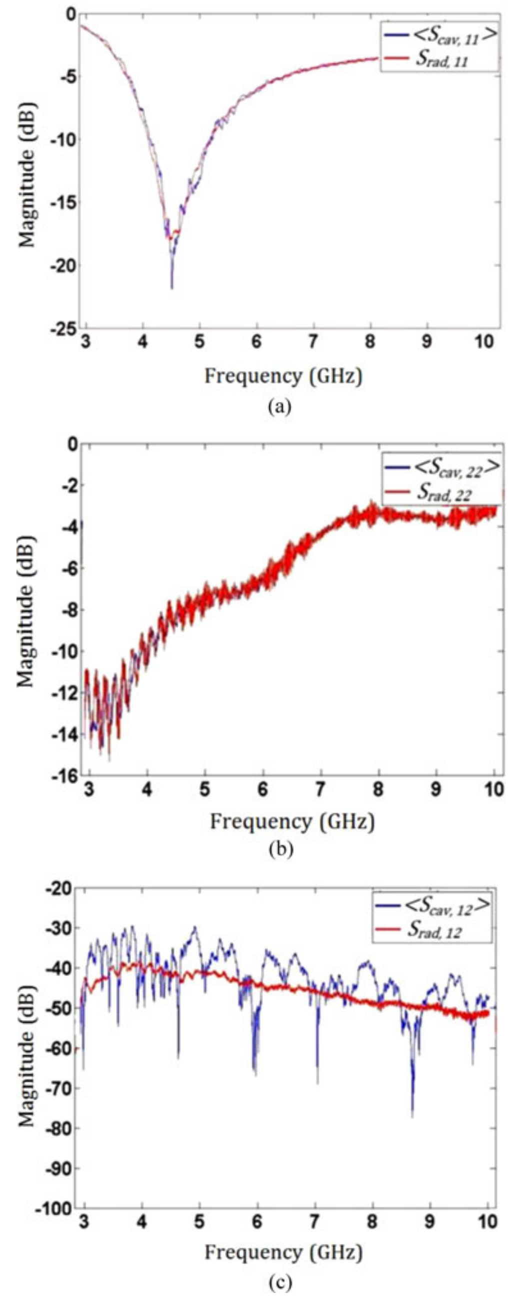

Fig. 4. $\boldsymbol{S}_{\rm rad}$ and $\langle \boldsymbol{S}_{\rm cav} \rangle$ comparisons. Fig. 4 (a), (b), and (c) shows comparisons of $\boldsymbol{S}_{\rm rad}$ and $\langle \boldsymbol{S}_{\rm cav} \rangle$ for S_{11}, S_{22}, and S_{12}, respectively.

C. Comparison of RCM PDFs and Experimental PDFs of the Induced Voltages on the Conductor in the GigaBox

We have shown that the RCM can well describe the universal fluctuating feature and the system-specific feature of the impedance matrix (or the scattering matrix) of a complex enclosure. Now we consider the application to the induced voltage on the long port. We imagine that a pulse of electromagnetic energy enters the enclosure through port 1, and we wish to estimate the distribution of voltages present on port 2. The PDF of induced voltages on port 2 is valuable information for assessing the risks of electromagnetic interference on the electrically long

$$\boldsymbol{Z}_{cav} \xrightarrow{average} \langle \boldsymbol{Z}_{cav} \rangle_{200} \xrightarrow{(3)} \boldsymbol{z} \xrightarrow{(5)} \alpha$$

Fig. 5. Process to obtain α from raw cavity impedance matrices.

$$\alpha \xrightarrow{(6)} \boldsymbol{z}_{RMT} \xrightarrow{(2)} \boldsymbol{Z}_{predicted}$$

Fig. 6. Process to obtain numerically generated impedance ensembles.

port, which represents a long cable in an enclosure. The PDF of induced voltages on a port can be directly obtained from experimental measurement of the impedance matrices from the 200 configurations of the GigaBox [9]. However, it is interesting to see if this PDF can be predicted numerically using the RCM for several frequency windows.

For a given frequency window, the loss parameter α, and the ensemble-averaged impedance matrix $\langle \boldsymbol{Z}_{\rm cav} \rangle$ of the GigaBox, were determined experimentally; see Fig. 5.

The loss parameter was then used to generate an ensemble of random normalized impedances, $\boldsymbol{z}_{\rm RMT}$, using the RMT. The ensemble of $\mathbf{z}_{\rm RMT}$, which were generated by the Monte Carlo method [see (6)], and the $\langle \boldsymbol{Z}_{\rm cav} \rangle$ of the GigaBox, which is solely a property of the ports, were used to predict the ensemble of theoretical impedance by using (2) and replacing $\boldsymbol{z}$ with $\boldsymbol{z}_{\rm RMT}$; see Fig. 6.

From this ensemble of numerically generated impedance, the numerical PDF of the induced voltages was generated [9].

In the experiments, both ports were connected to the network analyzer for measurement of the scattering matrix. In that case, the ports are terminated with the characteristic impedance (50 Ω), and therefore, no reflection comes back from the transmission lines. In practice, there may be a load impedance, Z_L, on port 2, and the voltages induced on that port may be generated by directly using the measured cavity impedance without any numerically generated normalized impedance, z, utilizing [11]

$$|V| = \left| \sqrt{\frac{2P_1(f)|Z_p|^2 |Z_{11}^{\rm cav}|^2}{{\rm Re}[Z_{11}^{\rm cav}]}} \right| \tag{7}$$

where

$$Z_p = \frac{Z_{21}^{\rm cav} Z_L / Z_{\rm eq}}{Z_{22}^{\rm cav} + Z_L} \text{ and } Z_{\rm eq} = Z_{11}^{\rm cav} - \frac{Z_{21}^{\rm cav} Z_{21}^{\rm cav}}{Z_{22}^{\rm cav} + Z_L}. \tag{8}$$

The radiated power spectrum of port 1, $P_1(f)$, is assumed to be constant in frequency windows of 100-MHz bandwidth. We may also assume a special case that the load impedance Z_L on port 2 approaches infinity (open circuit on port 2). In this case, the experimental PDFs of the induced voltages $|V|$ may be calculated as

$$|{\rm V}| = \left| \sqrt{\frac{2P_1(f)|Z_{21}^{\rm cav}|^2}{{\rm Re}[Z_{11}^{\rm cav}]}} \right|. \tag{9}$$

Here, we demonstrate results from four different frequency windows, which have their own distinct loss parameter value. These are 3.0–3.1 GHz (with $\alpha = 1.24$), 5.0–5.1 GHz (with $\alpha = 2.33$), 7.0–7.1 GHz (with $\alpha = 6.19$), and 10.0–10.1 GHz (with $\alpha = 10.93$). Fig. 7 shows the comparison of the PDFs of induced voltages, $P(|V|)$, computed experimentally and numerically by (7) and (8) with $Z_L = 50\ \Omega$ for these four frequency windows, respectively. For each numerical curve, we use the Monte Carlo method [see (6)] to generate 2×10^6 impedance matrix samples of $\boldsymbol{z}_{\rm RMT}$. The agreement between the experimental PDFs and the numerical RCM PDFs is very good. This is good evidence that the RCM successfully predicts the probability of induced voltages in this cavity, and it even works for an electrically large port.

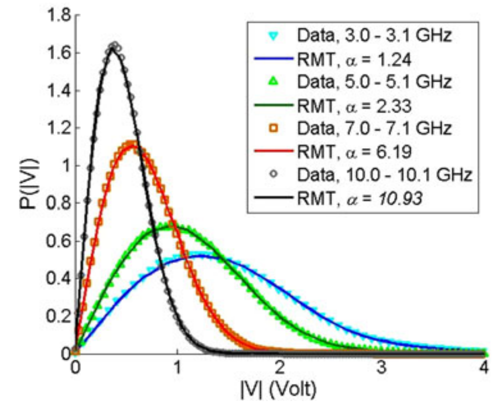

Fig. 7. Comparison of numerical RCM PDFs and experimental PDFs of the induced voltages on port 2 in frequency windows: 3.0–3.1 GHz (with $\alpha = 1.24$), 5.0–5.1 GHz (with $\alpha = 2.33$), 7.0–7.1 GHz (with $\alpha = 6.19$), and 10.0–10.1 GHz (with $\alpha = 10.93$).

D. Independence of Voltage Distributions on Port Locations

The distribution of the induced voltages on the target (port 2) should be independent of the location of the energy transmitting source (port 1), when the off-diagonal components of $\langle \boldsymbol{Z}_{\rm cav} \rangle$ are negligible compared to the diagonal components of $\langle \boldsymbol{Z}_{\rm cav} \rangle$ according to (4) [11]. For example, this is true when the ports are far apart or the major short trajectories are blocked. Also, the distribution should be independent of source locations because the E-fields in the cavity (as a reverberation chamber), due to the ray-chaotic nature, should have random polarizations and incidences resulting in similar distributions.

An experiment was carried out to investigate this hypothesis. The monopole antenna at port 1 was moved from its original location to the alternative location, which is also shown in Fig. 1 (which is 0.3 m away from the original location of port 1 horizontally, and 0.076 m away vertically). We plot the PDFs of induce voltages computed experimentally by (9) setting $Z_L \to \infty$. Fig. 8 shows little difference in the results of the measured PDFs of induced voltage from 8.0 to 8.1 GHz. This demonstrates that the statistics of induced voltage are dictated by a single property of the enclosure—the loss parameter, in addition to the radiation impedance matrix of the ports (or the ensemble-averaged impedance matrix of the ports [17], [18]).

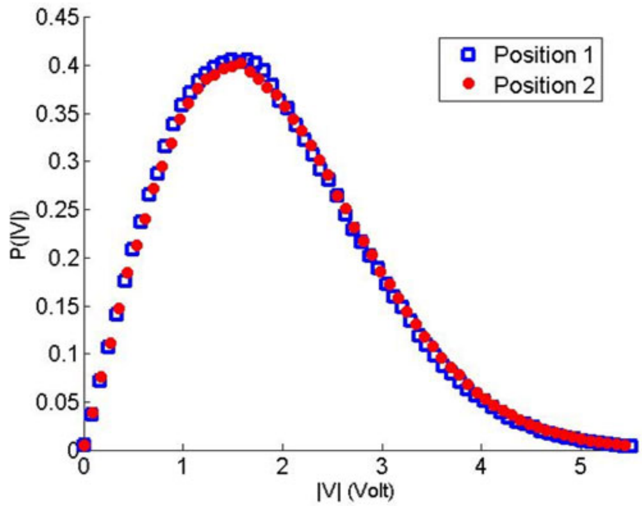

Fig. 8. Comparison of PDFs of the induced voltages on port 2 measured with the source monopole at the original location of port 1 (blue squares) and at the alternative location of port 1 (red dots) from 8.0 to 8.1 GHz.

V. Conclusion

The experimental results demonstrate that the RCM can be applied to a large, 3-D enclosure, which has an electrically large port, for statistical predictions of electromagnetic fields. The applicability of the RMT to the 3-D cavity is also verified. The existence of universal fluctuations in the 3-D cavity was shown through experimental results. The ability to obtain $\langle \boldsymbol{Z}_{\text{cav}} \rangle$ by averaging the measured cavity impedance matrices $\boldsymbol{Z}_{\text{cav}}$ avoids the impractical free space measurement of large and complicated cavities. We examined the radiation scattering matrix $\boldsymbol{S}_{\text{rad}}$ of the 3-D enclosure, which should follow the trend of the ensemble-averaged scattering matrix $\langle \boldsymbol{S}_{\text{cav}} \rangle$ as in previous RCM research [17], [18]. In this paper, we focused on $\langle \boldsymbol{S}_{\text{cav}} \rangle$, which better describes the system-specific features of the wave enclosure. We summarized the RCM process of utilizing the experimental data to obtain the loss parameter α (in Fig. 5) and the RCM process of generating numerical predictions of $\boldsymbol{Z}_{\text{cav}}$ by α and $\langle \boldsymbol{Z}_{\text{cav}} \rangle$ (in Fig. 6). PDFs of the induced voltages on the electrically large port in the cavity, which are numerically calculated by the RCM, closely match their experimental PDF counterparts.

For generating the numerical predictions by the RCM, one needs to determine the loss parameter of the system, and the system-specific features as $\langle \boldsymbol{Z}_{\text{cav}} \rangle$. In this paper, we used the 200 measured $\boldsymbol{Z}_{\text{cav}}$ realizations to determine the loss parameter (in Section III-B) and to calculate $\langle \boldsymbol{Z}_{\text{cav}} \rangle$ (in Section IV-B). It is worth noting that there are alternative ways to determine these two factors. For example, the loss parameter can be calculated directly from first principles with the quality factor as (4). For the ensemble-averaged impedance matrix $\langle \boldsymbol{Z}_{\text{cav}} \rangle$, Hart *et al.* [17], [18] have introduced the short-trajectory correction to synthesize the approximation of $\langle \boldsymbol{Z}_{\text{cav}} \rangle$ by utilizing the geometry of the enclosure.

The prediction of induced voltage on the conductor is also shown to be independent of the transmitting port location. Therefore, once the loss parameter is determined, it can be applied when the enclosure configuration is changed. This condition is constrained to the case of uniform loss in the enclosure. Future RCM work will focus on external radiation into a large cavity with an aperture. The introduction of large apertures, which become the dominant source of loss in the enclosure, would cause the voltage distributions due to different transmitting locations to deviate.

References

[1] D. A. Hill, *Electromagnetic Fields in Cavities: Deterministic and Statistical Theories*, New York, NY, USA: Wiley, 2009.

[2] D. Fedeli, G. Gradoni, V. M. Primiani, and F. Moglie, "Accurate analysis of reverberation field penetration into an equipment-level enclosure," *IEEE Trans. Electromagn. Compat.*, vol. 51, no. 2, pp. 170–180, May 2009.

[3] Y. He and A. C. Marvin, "Aspects of field statistics inside nested frequency-stirred reverberation chambers," in *Proc. IEEE Int. Symp. Electromagn. Compat.*, Austin, TX, USA, Aug. 2009, pp. 171–176.

[4] G. B. Tait, R. E. Richardson, M. B. Slocum, M. O. Hatfield, and M. J. Rodriquez, "Reverberant microwave propagation in coupled complex cavities," *IEEE Trans. Electromagn. Compat.*, vol. 53, no. 1, pp. 229–232, Feb. 2011.

[5] G. B. Tait, C. Hager, M. B. Slocum, and M. O. Hatfield, "On measuring shielding effectiveness of sparsely moded enclosures in a reverberation chamber," *IEEE Trans. Electromag. Compat.*, vol. 55, no. 2, pp. 231–240, 2013.

[6] H.-J. Stockmann, *Quantum Chaos: An Introduction*, Cambridge, U.K.: Cambridge Univ. Press, 1999.

[7] R. Holland and R. St. John, *Statisttical Electromagnetics*, Phildelphia, PA, USA: Taylor & Francis, 1999.

[8] R. S. Langley, "A reciprocity approach for computing the response of wiring systems to diffuse electromagnetic fields," *IEEE Trans. Electromagn. Compat.*, vol. 52, no. 4, pp. 1041–1055, Nov. 2010.

[9] S. Hemmady, "A wave-chaotic approach to predicting and measuring electromagnetic field quantities in complicated enclosures," Ph. D. Thesis, Univ. of Maryland, College Park, MD, USA, 2006.

[10] S. Hemmady, X. Zheng, H. Hart, T. M. Antonsen Jr., E. Ott, and S. M. Anlage, "Universal properties of two-port scattering, impedance, and admittance matrices of wave-chaotic systems," *Phys. Rev. E*, vol. 74, 2006.

[11] S. Hemmady, T. M. Antonsen, E. Ott, and S. M. Anlage, "Statistical prediction and measurement of induced voltages on components within complicated enclosures: A wave-chaotic approach," *IEEE Trans. Electromagn. Compat.*, vol. 54, no. 4, pp. 758–771, Aug. 2012.

[12] G. Gradoni, J.-H. Yeh, B. Xiao, T. M. Antonsen, S. M. Anlage, and E. Ott, "Predicting the statistics of wave transport through chaotic cavities by the random coupling model: A review and recent progress," *Wave Motion*, vol. 51, pp. 606–621, 2014.

[13] E. Ott, *Chaos in Dynamical Systems*, Cambridge, U.K.: Cambridge Univ. Press, 1993.

[14] M. L. Mehta, *Random Matrices*, San Diego, CA, USA: Academic, 1991.

[15] X. Zheng, T. M. Antonsen Jr., and E. Ott, "Statistics of impedance and scattering matrices of chaotic microwave cavities: Single channel case," *Electromagnetics*, vol. 26, pp. 3–35, 2006.

[16] X. Zheng, T. M. Antonsen Jr., and E. Ott, "Statistics of impedance and scattering matrices of chaotic microwave cavities with multiple ports," *Electromagnetics*, vol. 26, pp. 37–55, 2006.

[17] J.-H. Yeh, J. Hart, E. Bradshaw, T. M. Antonsen, E. Ott, and S. M. Anlage, "Universal and non-universal properties of wave-chaotic systems," *Phys. Rev. E*, vol. 81, 2010.

[18] J. A. Hart, T. M. Antonsen, and E. Ott, "The effect of short ray trajectories on the scattering statistics of wave-chaotic systems," *Phys. Rev. E*, vol. 80, 2009.

[19] R. H. Price, H. T. Davis, and E. P. Wenaas, "Determination of the statistical distribution of electromagnetic field amplitudes in complex cavities," *Phys. Rev. E*, vol. 48, no. 6, pp. 4716–4729, 1993.

[20] X. Zheng, S. Hemmady, T. M. Antonsen, S. M. Anlage, and E. Ott, "Characterization of fluctuations of impedance and scattering matrices in wave chaotic scattering," *Phys. Rev. E*, vol. 73, 2006.

Zachary B. Drikas (S'07–M'13) received the B.S. and M.S. degrees in electrical engineering in 2011 and 2012, respectively, from the George Washington University, Washington, DC, USA.

He is currently with the High Power Microwave Section, U.S. Naval Research Laboratory, Washington, where his research interests include investigating high-power microwave effects on electronics, nonlinear behavior in semiconductors, electromagnetic time-reversal techniques, and using the random coupling model to characterize and predict effects on targets in ray-chaotic enclosures. He has coauthored peer-reviewed publications on the random coupling model and electromagnetic time-reversal techniques, and he has given numerous presentations at the annual symposium of the directed energy professional society.

Jesus Gil Gil received the B.S. and M.S. degrees both in electrical engineering from George Mason University, Fairfax, VA, USA, in 2005 and 2008, respectively.

He is currently an Electrical Engineer in the High Power Microwave Section, U.S. Naval Research Laboratory, Washington, DC, USA. His research interests include chaos in electronics, the random coupling model, metamaterials, nonlinear behavior in semiconductors, and high-power Microwaves. He has coauthored peer-reviewed publications on the random coupling, and he has given numerous presentations at the annual symposium of the directed energy professional society.

Sun K. Hong (S'06–M'10) received the B.S. degree in electrical engineering from the University of Maryland, College Park, MD, USA, in 2005, and the M.S. and Ph.D. degrees in electrical engineering from Virginia Tech, Blacksburg, VA, USA, in 2008 and 2012, respectively.

He is currently a Researcher in the Tactical Electronic Warfare Division, U.S. Naval Research Laboratory, Washington, DC, USA. His current research interests include time-reversal techniques in electromagnetics, nonlinear metamaterials, and transient scattering techniques, as well as target identification. Some of his recent/past involvement includes HPM effects, antenna design for HPM application and UWB measurements, and biomedical applications.

Dr. Hong is a member of Eta Kappa Nu. He is a Visiting Scholar in the Ultrafast and Nonlinear Photonics Lab, Johns Hopkins University, Baltimore, MD.

Tim D. Andreadis received the B.S. degree in physics and the Ph.D. degree in nuclear engineering, in 1974 and 1981, respectively, both from the University of Maryland, College Park, MD, USA.

He is currently the Head of the High Power Microwave section, U.S. Naval Research Laboratory, Washington, DC, USA. The HPM section is engaged in work that includes research on HPM effects on electronics, counter IED applications, high-power RF source applications, and electromagnetic backscatter. He has an extensive list of peer reviewed publications, conference proceedings, and reports. He has numerous invited talks and presentations at national and international conferences.

Dr. Andreadis is a Fellow and the President of the Directed Energy Professional Society

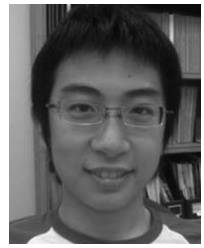

Jen-Hao Yeh received the Bachelor of Science degree (2006) in electrical engineering and physics (double major) from National Taiwan University, Taipei, Taiwan, the Ph.D. degree in electrical and computer engineering from the University of Maryland, College Park, MD, USA, in 2013.

He is currently a Research Associate in the Laboratory for Physical Sciences, studying the field of superconducting quantum computing University of Maryland. He is also an Electrical Engineer in microwave engineering with expertise in statistical electromagnetism and wave chaos. During Ph.D. research, he was advised by Prof. S. Anlage (ECE). They collaborated with Prof. T. Antonsen (ECE), Prof. E. Ott (ECE), and their students as a Wave Chaos Group. This group studies varied topics related to wave chaos, wave phenomenon in a chaotic boundary condition. His research interests include experimental verification of the random coupling model and applications on real-world wave propagation issues, such as fading and high-power microwave effects.

Biniyam T. Taddese (S'11) received the Graduate summa cum laude degree with the B.A. degree majoring in physics, computer science, and mathematics from Macalester College, St. Paul, MN, USA, in 2006, and the M.S. and the Ph.D. degrees in electrical engineering from the University of Maryland, College Park, MD, USA, in 2010 and 2012, respectively.

His current research interests include time reversed wave propagation, wave chaos, nonlinear dynamics, signal processing, and electromagnetic compatibility problems.

Steven M. Anlage (M'94) received the B.S. degree in physics from Rensselaer Polytechnic Institute, Troy, NY, USA, in 1982, and the M.S. and Ph.D. in applied physics from the California Institute of Technology, Pasadena, CA, USA, in 1984 and 1988, respectively.

He is currently a Professor of physics and the Faculty Affiliate of the Department of Electrical and Computer Engineering, University of Maryland, College Park, MD, USA. His graduate work concerned the physics and materials properties of quasicrystals. His post-doctoral work with the Beasley–Geballe–Kapitulnik group at Stanford University, Stanford, CA (1987–1990), concentrated on high-frequency properties of high temperature superconductors, including both basic physics and applications to tunable microwave devices. In 1990, he was appointed as an Assistant Professor of physics in the Center for Superconductivity Research at the University of Maryland, then in 1997 an Associate Professor, and finally, in 2002 a Full Professor of physics. He was the interim Director of the Center for Nanophysics and Advanced Materials (2007–2009), and is a Member of the Maryland NanoCenter. There his research in high frequency superconductivity has addressed questions of the pairing state symmetry of the cuprate superconductors, the dynamics of conductivity fluctuations and vortices, and microwave applications such as superconducting negative index of refraction metamaterials. He has also developed and patented a near-field scanning microwave microscope for quantitative local measurements of electronic materials (dielectrics, semiconductors, metals, and superconductors) down to nanometer length scales. He also performs microwave analog experiments of the Schrödinger equation to test fundamental theories of quantum chaos. As part of this work, he has developed a statistical prediction model for effects of high-power microwave signals on electronics. He is also active in the emerging field of time-reversed electromagnetics. In 2008, he was appointed as a Research Professor of the National Security Institute, Naval Postgraduate School, Monterey, CA. In 2011, he joined the Center for Functional Nanostructures, Karlsruhe Institute of Technology, Karlsruhe, Germany, as a Visiting Professor. He has coauthored more than 150 research papers in scientific journals.

Dr. Anlage is a Member of the American Physical Society, the Optical Society of America, and the Materials Research Society. His research is funded by the National Science Foundation, DoE and DoD, and he is an active consultant to the U.S. Government. He was a Member of the NSF-funded Materials Research Science and Engineering Center at the University of Maryland from 1995 to 2005